Propofol decreases spike firing frequency with an increase in cortical spike synchronization and a modulation in spike regularity

Mie Kajiwara
Nihon University Graduate School of Dentistry
Major in Anesthesiology
(Directors: Profs. Yoshiyuki Oi and Masayuki Kobayashi,
and Assist. Prof. Yuko Koyanagi)

Index

This thesis is based on the following article and additional results in terms of the effect of propofol on the regularity of spike firing (Fig. 7):

Mie Kajiwara, Risako Kato, Yoshiyuki Oi, Masayuki Kobayashi (2020)
Propofol decreases spike firing frequency with an increase in spike synchronization in the cerebral cortex. Journal of Pharmacological Sciences. 142:83-92.

Abstract

Little is known about how propofol modulates the spike firing correlation between excitatory and inhibitory cortical neurons *in vivo*. The extracellular unit recordings were performed from rat insular cortical neurons, and the recorded neurons were classified with high spontaneous firing frequency, bursting, and short spike width as high frequency with bursting neurons (HFB; pseudo fast-spiking GABAergic neurons) and other neurons with low spontaneous firing frequency and no bursting were classified as non-HFB. Intravenous administration of propofol (12 mg/kg) from the tail vein reduced the firing frequency of HFB, whereas propofol initially increased (within 30 s) and then decreased the firing frequency of non-HFB. Both HFB and non-HFB spontaneous action potential discharge was depressed by propofol with a greater depression seen for HFB. Cross-correlograms and auto-correlograms demonstrated propofol-induced increases in the ratio of the peak, which were mostly observed around 0-10 ms divided to baseline amplitude. The analysis of interspike intervals showed a decrease in spike firing at 20-100 Hz and a relative increase at 8-15 Hz. Furthermore, spike firings were transformed by unfolding transformation based on random matrix theory to evaluate their regularity. Propofol decreased the number of both HFB and non-HFB with repulsion and increased the number of non-HFB fitted to an exponential function, suggesting that regularity of spike timing is maintained in HFB rather than in non-HFB after propofol injection. These results suggest that propofol induces a larger suppression of firing frequency in HFB and an enhancement of synchronized neural activities in the α frequency band in the cerebral cortex.

Introduction

The cerebral cortex is one of the major targets for general anesthetics. Cerebrocortical neurons are divided into excitatory glutamatergic neurons and inhibitory GABAergic neurons. Excitatory pyramidal neurons are principal excitatory neurons projecting not only to other cortical regions but also to subcortical areas. Although GABAergic neurons occupy the minor population of cortical neurons,[1] neural activities of pyramidal neurons are potently regulated by inhibitory inputs from cortical GABAergic interneurons.[2] Therefore, to elucidate the brain state's transition mechanisms from conscious to unconscious by general anesthesia, it is critical to estimate the potency of general anesthetics affecting these excitatory and inhibitory neurons, i.e. the excitatory-inhibitory balance.[3]

Cortical GABAergic inhibitory neurons are classified into several subtypes by their immunohistochemical markers, such as parvalbumin, somatostatin, vasoactive intestinal polypeptide, and cholecystokinin, and electrophysiological features.[4] Expression of immunohistochemical markers correlates with the repetitive firing patterns responding to a long depolarizing current pulse injection. Parvalbumin-immunopositive cells, which occupy the largest population of cortical GABAergic neurons, show non-adapting firing at high-frequencies (fast-spiking; FS) with short spike duration, whereas somatostatin-immunopositive cells show regular spiking or burst spike firing.[4] Among these GABAergic neurons, FS neurons are the principal inhibitory neurons that potently suppress excitatory neuronal activities by inducing large inhibitory postsynaptic currents (IPSCs).[4-6]

Propofol, one of the representative intravenous anesthetics, potentiates the inhibition of neural activities by increasing Cl^- currents via $GABA_A$ receptors in cortical neurons.[7] The propofol-induced potentiation of GABAergic currents is induced by increasing the open probability of $GABA_A$ receptors[8] and thus prolonging the decay phase of IPSCs.[9,10] Among inhibitory connections in the cerebral cortex, the connections from FS neurons to pyramidal neurons exhibit the largest propofol-induced facilitation of IPSCs.[10]

Cortical $GABA_A$ receptors induce persistent tonic Cl^- currents,[11] and propofol enhances the tonic Cl^- currents, which modulate the passive membrane and firing properties.[12] In addition to changing the kinetics of $GABA_A$ receptors, propofol modulates intrinsic neuronal properties such as action potential induction[12,13] and input resistance.[12] These effects of propofol on ionic channels and receptors in cortical neurons are different among neuronal subtypes: the degree of the propofol-induced changes in the membrane and firing properties is more potent in pyramidal neurons than in FS neurons.[12]

To understand the mechanisms of propofol-induced anesthesia, it is necessary to examine the modulatory profiles of spontaneous spike firing of excitatory and inhibitory

cortical neurons by propofol. Using extracellular unit recording with multi-electrodes, the recorded cortical neurons were classified into high frequency with bursting neurons (HFB), presumably GABAergic FS neurons, and non-HFB, and the synchronization of neural discharge by propofol was examined among HFB and non-HFB.

Materials and Methods

All experiments were performed in accordance with the National Institutes of Health Guide for the Care and Use of Laboratory Animals and were approved by the Institutional Animal Care and Use Committee at Nihon University. All efforts were made to minimize the number and suffering of animals used in experiments.

Animals

Experimental procedures were similar to that described previously.[14] Briefly, eight-week-old Wistar rats (n = 58, male, Japan SLC) were used. Lightweight head attachments (Narishige, Tokyo, Japan) were attached after habituation under 2.0-2.5% isoflurane anesthesia (Pfizer, Tokyo, Japan). In addition, the screws were set on the frontal cortex (2.5 mm anterior and 2.0 mm lateral to the bregma) and the cerebellum, which were used as an electrode (10 kΩ) for electroencephalogram (EEG) recording and for grounding respectively. The depth of anesthesia was determined by the absence of the hindlimb pinch reflex. The body temperature was monitored using a rectal probe (BWT-100, Bio Research Center, Japan) and maintained at approximately 37°C using a heat pad. Rats received analgesia (carprofen, 5 mg/kg, s.c., Zoetis, Tokyo, Japan) and maintenance medium (10 ml, s.c., Sorita-T3, Ajinomoto, Tokyo, Japan) during the surgery.

Unit recording

On a recording day, the habituated rats received a small craniotomy and an incision of the dura mater under general anesthesia with 2.0% isoflurane. Ropivacaine hydrochloride (AstraZeneca, Osaka, Japan) was applied to the incisions. After recovery from anesthesia, the unit recording was performed.

After setting the rats to the frame, the microelectrode arrays (A1x32-Poly3-10mm-50-177, NeuroNexus, Ann Arbor, USA) with 32 circular electrodes (Fig. 1A) were perpendicularly inserted 0.7 mm anterior and 5.2 mm lateral to the bregma and 3.8-4.6 mm from the cortical surface using a step-by-step protocol. Under the awake condition, extracellular recordings (10-30 min) were performed from neurons in layers II-VI of the left insular cortex (IC; Fig. 1B), which receives somatosensory inputs from oral structures.[15] Twelve mg/kg propofol (Aspen, Tokyo, Japan) was then intravenously injected via the tail vein. The duration of injection was approximately 30 s. During both the awake and anesthetized conditions, recordings were obtained from the same neurons.

The action potentials were recorded extracellularly, amplified, filtered, and digitized using a Plexon Recorder System (band pass: 100 Hz-8 kHz; sampling rate 31.25 kHz; Plexon,

Dallas, USA).

After recording, fixed cortical sections were stained with Cresyl violet to visualize the recording sites (Fig. 1B).

EEG recording

EEGs were simultaneously recorded using an amplifier (band pass: 1-300 Hz; ER-1, Cygnus Technology, Delaware Water Gap, USA). EEGs were digitized and stored on a computer hard disk using Micro 1401 MK2 (Cambridge Electronic Design, Cambridge, UK). Power spectrum analysis was performed using dedicated software (NeuroExplorer ver. 4, Plexon).

Spike analysis

The recorded spikes were sorted into single units based on the peak amplitude, the sum of the squared amplitude, and the half-width using Off-line Sorter software (ver. 3, Plexon).[14] The duration at the half-amplitude of the negative peak from the baseline was measured as the spike width. To distinguish burst episodes from isolated spikes, a burst episode was defined as any continuous group of two or more spikes (i) whose minimum interspike interval (ISI) was < 5 ms and (ii) whose maximum ISI was < 2.5 times the minimum ISI. Statistical calculations of spike firing and the power spectral density of spike firing were performed using Neuroexplorer (ver. 4.110, Nex Technologies, USA).

Cross-correlograms and autocorrelograms during propofol-induced anesthesia were obtained from recording between 1 and 10 min after propofol injection. The bin width and time range of cross-correlograms were set to 1 ms and -50 to 50 ms, respectively. The mean number of events between -5 to 5 ms was compared to that of -50 to -6 ms and 6 to 50 ms using Student's *t*-test. The ratio of the peak, which were mostly observed around 0-10 ms, divided to baseline amplitude was defined as P/B ratio.

RMT analysis

To detect the regularity of neural firing, spike firing was transformed by unfolding transformation based on random matrix theory (RMT).[14] This procedure makes it possible to define an average spike interval locally in time and to compare different activity states on a universal scale, which distinguish whether events involve regularity. This procedure removes the system-specific average spike density. According to the methods described by Kato et al.,[14] the spike train was examined whether the unfold histograms have repulsion and which decay function – exponential or power – fits the histograms.

Statistics

The data are expressed as the mean ± SEM. Comparisons of the firing frequency between awake and anesthetized conditions were conducted using a paired *t*-test. Student's *t*-test was used to compare the firing frequency between HFB and non-HFB. In the cases without normal distributions and equal variances, Mann-Whitney U test was used for the comparisons. Correlations between variables were evaluated with the non-parametric Spearman Rho tests. Statistical analyses were performed using a software (OriginPro 8J, Northampton, USA). $P < 0.05$ was considered significant.

Results

Classification of recorded neurons

In reference to the characteristics of FS neurons, i.e. short spike width, high spike frequency, and the large number of spikes within a burst (NSB), the extracellularly recorded neurons were classified into two subtypes, i.e. HFB and non-HFB (Fig. 1C-E).[14,16] HFB fulfilled all criteria of: (1) high spontaneous firing frequencies (> 5 Hz); (2) large NSB max (> 5); and (3) short spike width (n = 34; Fig. 1C,E).[14] On the other hand, non-HFB were defined by a spike width longer than 150 μs and with firing frequencies mostly lower than 10 Hz (n = 305; Fig. 1D,E). Thus, HFB and non-HFB were considered to be FS neurons and non-FS neurons.

Non-HFB showed a lower spontaneous firing frequency ($P < 0.001$, Mann-Whitney U test; Fig. 1Fa). Spike width was shorter in HFB than non-HFB ($P = 0.002$, Mann-Whitney U test; Fig. 1Fb). The maximum number of spikes within each burst was larger in HFB in comparison to that in non-HFB ($P < 0.001$, Mann-Whitney U test; Fig. 1Fc).

Propofol reduces spontaneous firing frequency

Fig. 2A, B shows an example of simultaneous recordings from HFB and non-HFB before and after an intravenous injection of 12 mg/kg propofol to the tail vein. Just after the injection of propofol, non-HFB showed a temporal increase in spontaneous spike firing (Fig. 2B, arrow), whereas HFB showed little change. The temporal increase in firing frequency in non-HFB was sustained for 30 s. After the initial increase in the firing frequency, non-HFB showed a gradual decrease, which occurred parallel to that in HFB (Fig. 2A,B, arrowheads).

A shot injection of propofol induced a rapid suppression of spontaneous spike firing in HFB (Fig. 2C) that continued up to 15 min after propofol injection. The firing rate (%) was compared to the mean spike firing rate during an awake state (5 min before propofol i.v.). HFB showed an abrupt decrease in the firing rate within 10 s followed by a suppression of spike firing sustained for ~10 min. After the suppression of spike firing, the firing rate gradually increased. The spike firing rate reached its lowest point 1 min after propofol i.v. (Fig. 2C).

Non-HFB showed a different change in firing rate: non-HFB initially increased their firing rate at the first bin (bin width = 5 s; Fig. 2D). After the initial increase in spike firing, the firing rate decreased beyond the baseline rate. During this period (0.5-1.0 min), the firing rate of non-HFB was significantly larger than that of HFB (Fig. 2C). The firing rate of non-HFB reached the minimum 3.5 min after propofol i.v. (Fig. 2C). Up to 15 min after propofol i.v., non-HFB showed a smaller suppression rate of the firing rate in comparison to

HFB ($P < 0.05$-0.001, Student's *t*-test; Fig. 2C).

To confirm that propofol injections induce anesthetized conditions, EEGs were recorded from the parietal part of the cortex as shown in Fig. 2E. As previously reported,[17] propofol injections increased the amplitude of EEG activities, and the analysis of power spectral density revealed an enhancement of α-band power spectral density (Fig. 2F). These EEG findings suggest that the propofol injection protocol reliably induced anesthetized conditions.

Cross-correlation between HFB and non-HFB pairs

The cross-correlograms obtained from 221 pairs of HFB and non-HFB were classified into two groups. The first group showed synchronized spike firing between -5 to 5 ms in the histograms: simultaneous spike firing (SSF) group (Fig. 3A left). The second group showed no significant peaks between -50 to 50 ms in asynchronized spike firing (ASF) group (Fig. 3B left). Among 221 pairs, 24.0% and 76.0% pairs were classified into SSF and ASF groups, respectively.

A typical example of the changes in cross-correlograms induced by propofol in the SSF group is shown in Fig. 3A. Propofol increased P/B ratio of SSF group ($n = 53$, $P < 0.001$, paired *t*-test; Fig. 4A left).

In the ASF group, 28.6% of pairs showed a propofol-induced enhancement of synchronized spike firing. A typical example is shown in Fig. 3B. In sum, propofol significantly increased P/B ratio in ASF group ($n = 168$, $P < 0.001$, paired *t*-test; Fig. 4A right). These results suggest that propofol enhances synchronization of HFB and non-HFB activities in parallel to decrease their firing frequency regardless of whether their firings were synchronous or asynchronous in the awake condition.

The relationship between P/B ratios during awake and propofol-induced anesthetized conditions is shown in Fig. 4B. There was a significant correlation between them ($r^2 = 0.696$, $P < 0.001$, Spearman Rho test; Fig. 4B), suggesting that higher synchronized HFB and non-HFB pairs show a larger increase in the synchronized activities.

Cross-correlation between HFB and HFB pairs

Fig. 3C, D shows typical examples of the cross-correlograms between HFB and HFB of SSF and ASF group. Propofol tended to increase P/B ratio in the SSF group ($n = 4$; Fig. 4D left), and significantly increased P/B ratio in the ASF group ($n = 12$, $P = 0.03$, paired *t*-test; Fig. 4D right). The significant correlation between P/B ratios during awake and propofol-induced anesthetized conditions is shown in Fig. 4E ($r^2 = 0.972$, $P < 0.001$, Spearman Rho test).

Cross-correlation between non-HFB and non-HFB pairs

Fig. 3E, F shows typical examples of the cross-correlograms between non-HFB and non-HFB of SSF and ASF group, respectively. Propofol significantly increased P/B ratios in the SSF (n = 112, $P < 0.001$, paired *t*-test; Fig. 4G left) and ASF groups (n = 420, $P < 0.001$, paired *t*-test; Fig. 4G right). The significant correlation between P/B ratios during awake and propofol-induced anesthetized conditions is shown in Fig. 4H ($r^2 = 0.258$, $P < 0.001$, Spearman Rho test).

Correlation between the distance of neurons and P/B ratio

Further analysis of the relationship between the distance of HFB and non-HFB, HFB and HFB, and non-HFB and non-HFB, and the enhancement of P/B ratio by propofol was performed. There was no significant correlation between these parameters: $r^2 = -0.004$ in HFB and non-HFB ($P = 0.847$, Spearman Rho test; Fig. 4C), $r^2 = -0.032$ in HFB and HFB ($P = 0.476$, Spearman Rho test; Fig. 4F), and $r^2 = -0.001$ in non-HFB and non-HFB ($P = 0.60$, Spearman Rho test; Fig. 4I). These results suggest that propofol-induced enhancement of synchronized spike firing occurs in the whole IC rather than a restricted region in IC.

Auto-correlation analysis

To examine the effect of propofol on the spike firing interval in HFB and non-HFB, the auto-correlograms obtained from these neurons were compared. Auto-correlograms of HFB and non-HFB in the awake state both showed troughs with a minimum at 0 ms (count/bin = 0); however, they differ in shape (Fig. 5A,C,E). Auto-correlograms of HFB exhibited a V-shaped trough (Fig. 5A,C). Some of the HFB (n = 10/33, 30.0%) showed peaked auto-correlograms (PA type) and exhibited symmetric peaks in reference to 0 ms, meaning that a large part of spontaneous spikes occurred in a burst-mode in which the interspike interval is short (Fig. 5A). However, other HFB (n = 23/33, 70.0%) showed flattened auto-correlograms (FA type, Fig. 5C) rather than PA type. Conversely, non-HFB showed a U-shaped trough around 0 ms and no apparent peaks were observed (Fig. 5E), suggesting that spontaneous firing of non-HFB occurred almost randomly. In the awake condition, P/B ratio of HFB (1.6 ± 0.3, n = 33) was comparable to that of non-HFB (1.1 ± 0.1, n = 124, $P = 0.14$, Student's *t*-test).

Propofol changed the profiles of the auto-correlograms of both neural types (Fig. 5B,D,F). In terms of HFB, of both PA and FA types, P/B ratio was increased by propofol (n = 33, $P < 0.001$, paired *t*-test; Fig. 5G). This is also the case for P/B ratio of non-HFB (n = 124, $P < 0.001$, paired *t*-test; Fig. 5H).

In HFB, there was a significant correlation between P/B ratios during awake and

propofol-induced anesthetized conditions ($r^2 = 0.348$, $P < 0.001$, Spearman Rho test; Fig. 5I). In contrast, no significant correlation was observed between P/B ratios during awake and propofol-induced anesthetized conditions in non-HFB ($r^2 = 0.182$, $P = 0.72$, Spearman Rho test; Fig. 5J). These results suggest that propofol enhances burst-like spike firing both in HFB and non-HFB, and HFB with a higher P/B ratio are more potently enhanced by propofol.

Propofol-induced changes in interspike interval histograms

The cross- and auto-correlograms were skewed toward 0 ms by propofol, indicating that propofol induces synchronized spike firing and burst firing among HFB and non-HFB. However, these analyses cannot characterize the population of spike firing frequency, which may reflect an EEG feature. To approach this issue, ISI was analyzed in both awake and propofol-induced anesthetized conditions.

In the awake condition, the normalized histogram of ISI (1-200 ms) skewed toward a shorter ISI both in HFB and non-HFB (Fig. 6A,D). Peaks in the histograms of HFB and non-HFB were detected at 3 ms (Fig. 6A) and 4 ms (Fig. 6D), respectively. The amplitude of bins gradually and almost monotonically decreased down to 200 ms.

In HFB, propofol injections changed the profile of ISI histogram (Fig. 6B). To highlight the difference between the awake and propofol-induced anesthetized conditions' histograms, the awake ISI histogram was subtracted from the ISI histogram of propofol (Fig. 6C). The resulting histogram clearly showed that the amplitude of ISI mostly decreased during the short ISI (10-57 ms ISI), (n = 33, paired *t*-test; Fig. 6C) then slightly increased during the longer ISI (> 120 ms ISI). As a result, the ISI histogram of propofol exhibited the hump that appeared between ~50 ms and ~120 ms (Fig. 6B, inset arrowhead).

The decreased amplitude of the ISI histogram of propofol was also observed in non-HFB. The amplitude of the bin mostly decreased during the short ISI (12-58 ms ISI), (n = 126, paired *t*-test; Fig. 6D-F). However, non-HFB showed an increase in Δ frequency during the short ISI (3-8 ms), whereas they barely increased in Δ frequency during the long ISI (> 120 ms; Fig. 6F). As a result, the hump appeared between around 60-120 ms (Fig. 6E, inset arrowhead).

These results suggest that the high frequency of spike firing at around 20-100 Hz is decreased and spike firing at 8-15 Hz is increased in both HFB and non-HFB.

Effect of propofol on the regularity of spike firing

RMT makes it possible to distinguish the firing patterns with or without regularity: in the cases of no correlation between two adjacent spike timings, the distribution pattern of a plot is fitted by exponential decay without repulsion, whereas in the cases of close correlation of

spikes, the distribution pattern of a plot should be fitted by a power decay with repulsion.

Unfolding transformation demonstrated that both HFB and non-HFB showed a decrease in the number of neurons with repulsion by propofol injection (Fig. 7A). This suggests that propofol makes the correlation between a spike and subsequent spikes in short time scale weakened in both types of neurons.

Under the awake condition, the unfold histogram of HFB and non-HFB that were fitted with an exponential function, which means less correlation of the first spike with subsequent spikes, occupied 67.6% and 57.0%, respectively. On the other hand, under propofol-induced anesthetized conditions, the number of non-HFB fitted to an exponential function increased to 71.8%, but there was no change in HFB (Fig. 7B). These results suggest that regularity of spike timing is maintained in HFB rather than in non-HFB after propofol injection.

Discussion

In vivo whole-cell patch-clamp recordings have revealed that FS neurons show frequent spontaneous spike firing,[18] which matches the present criteria of HFB. On the other hand, non-HFB likely involve both glutamatergic excitatory neurons and a part of GABAergic inhibitory neurons. The population of cerebrocortical GABAergic neurons is around 20%,[1] and among the GABAergic neurons, parvalbumin-immunopositive neurons—which show FS firing—occupy about half population.[19] Taken together, this evidence indicates that most non-HFB are excitatory neurons.

Autapses are frequently observed in FS neurons in the cerebral cortex.[20] Therefore, in the initial phase, it is possible to postulate that a low dose of propofol predominantly suppresses FS neurons by enhancing GABAergic IPSCs mediated via autapses in comparison to pyramidal neurons. If this is the case, only FS neuronal activities decrease, which may induce a suppression of inhibitory inputs to pyramidal neurons via FS neurons. The disinhibition of pyramidal neurons possibly induces a temporal increase in pyramidal neuronal activities. The dissociation of spontaneous firing frequency could contribute to restlessness in the initial phase of general anesthesia. Propofol decreased regularity in non-HFB but not HFB although the firing frequency of HFB was significantly decreased by propofol injection. Autapses are also may contribute to maintain the regularity in HFB during propofol-induced anesthetized conditions.

The propofol-induced increase in P/B ratio of cross-correlogram between HFB and non-HFB suggests an enhancement of synchronized activities in IC neurons: HFB and non-HFB receive common excitatory inputs whose impact is strong enough to induce spike firing. Although the modulation of GABAergic currents and several ionic currents is likely to be involved in the propofol-induced suppression of cortical activities, such modulation cannot explain the enhancement of synchronization of spike firing.

One candidate of the origin of the large synchronized inputs is the thalamus. It has been reported that excitatory inputs via thalamocortical projections contribute to synchronizing cortical activity, which results in an enhancement of oscillations in the EEG.[21-23] The previous studies have reported that FS neurons in IC often exhibit autaptic currents,[10] which improve spike timing precision.[24] Therefore, HFB, presumably classified into FS and parvalbumin-immunopositive neurons, are likely to be regulated by autapses. Propofol increases $GABA_A$ receptor-mediated currents, and autapses are no exception to this effect. Thus, not only do the synchronized excitatory inputs from the thalamus contribute to the increase in synchronous activities among HFB and non-HFB, but the propofol-induced enhancement of autaptic currents may as well.

Electrical coupling via gap junctions and autapses are often observed in FS neurons.[5,10] Although propofol has little effect on the conductance of electrical synapses,[10] potentiation of autaptic currents may be involved in the suppression of the spontaneous firing rate in HFB. Synchronized activities of the membrane potential among FS neurons via gap junctions may increase synchronized oscillations cooperatively with autapses.

Unconsciousness induced by propofol is accompanied with frontal β oscillations (15-30 Hz) followed by α oscillations (8-13 Hz).[17,25] Several studies based on the EEG have demonstrated that both the cortex and thalamus play a critical role in the propofol-induced α-rhythm.[21,22] It is likely that the enhancement of P/B ratio in cross- and auto-correlograms reflect the enhancement of synchronization among HFB and non-HFB. In addition to the synchronized activities, the emergence of the hump in the ISI histograms observed around 50-120 ms (Fig. 6B,E) suggests the relative enhancement of the spike firing frequency at α-rhythm.

Acknowledgments

I am grateful to Prof. Yoshiyuki Oi for the opportunity to perform this study, Prof. Masayuki Kobayashi, Dr. Risako Kato, and Assist. Prof. Yuko Koyanagi for their instructions of this study, and colleagues in Department of Pharmacology for their technical advice and assistance.

References

1. Gabbott PL, Somogyi P. Quantitative distribution of GABA-immunoreactive neurons in the visual cortex (area 17) of the cat. *Exp Brain Res*. 1986;61:323-331.
2. Vizuete JA, Pillay S, Diba K, Ropella KM, Hudetz AG. Monosynaptic functional connectivity in cerebral cortex during wakefulness and under graded levels of anesthesia. *Front Integr Neurosci.* 2012;6:90.
3. Taub AH, Katz Y, Lampl I. Cortical balance of excitation and inhibition is regulated by the rate of synaptic activity. *J Neurosci.* 2013;33:14359-14368.
4. Kawaguchi Y, Kubota Y. GABAergic cell subtypes and their synaptic connections in rat frontal cortex. *Cereb Cortex.* 1997;7:476-486.
5. Koyanagi Y, Yamamoto K, Oi Y, Koshikawa N, Kobayashi M. Presynaptic interneuron subtype- and age-dependent modulation of GABAergic synaptic transmission by β-adrenoceptors in rat insular cortex. *J Neurophysiol.* 2010;103:2876-2888.
6. Kobayashi M, Takei H, Yamamoto K, Hatanaka H, Koshikawa N. Kinetics of $GABA_B$ autoreceptor-mediated suppression of GABA release in rat insular cortex. *J Neurophysiol.* 2012;107:1431-1442.
7. Kobayashi M, Oi Y. Actions of propofol on neurons in the cerebral cortex. *J Nippon Med Sch.* 2017;84:165-169.
8. Kitamura A, Sato R, Marszalec W, Yeh JZ, Ogawa R, Narahashi T. Halothane and propofol modulation of gamma-aminobutyric acid A receptor single-channel currents. *Anesth Analg.* 2004;99:409-415.
9. Kitamura A, Marszalec W, Yeh JZ, Narahashi T. Effects of halothane and propofol on excitatory and inhibitory synaptic transmission in rat cortical neurons. *J Pharmacol Exp Ther.* 2003;304:162-171.
10. Koyanagi Y, Oi Y, Yamamoto K, Koshikawa N, Kobayashi M. Fast-spiking cell to pyramidal cell connections are the most sensitive to propofol-induced facilitation of GABAergic currents in rat insular cortex. *Anesthesiology.* 2014;121:68-78.
11. Salin PA, Prince DA. Spontaneous $GABA_A$ receptor-mediated inhibitory currents in adult rat somatosensory cortex. *J Neurophysiol.* 1996;75:1573-1588.
12. Kaneko K, Koyanagi Y, Oi Y, Kobayashi M. Propofol-induced spike firing suppression is more pronounced in pyramidal neurons than in fast-spiking neurons in the rat insular cortex. *Neuroscience.* 2016;339:548-560.
13. Martella G, De Persis C, Bonsi P, Natoli S, Cuomo D, Bernardi G, Calabresi P, Pisani A. Inhibition of persistent sodium current fraction and voltage-gated L-type calcium current by propofol in cortical neurons: implications for its antiepileptic activity. *Epilepsia.*

2005;46:624-635.
14. Kato R, Yamanaka M, Yokota E, Koshikawa N, Kobayashi M. Spike timing rigidity is maintained in bursting neurons under pentobarbital-induced anesthetic conditions. *Front Neural Circuits.* 2016;10:86.
15. Kobayashi M, Horinuki E. Neural mechanisms of nociception during orthodontic treatment. *J Oral Sci.* 2017;59:167-171.
16. Kato R, Yamanaka M, Kobayashi M. Application of unfolding transformation in the random matrix theory to analyze *in vivo* neuronal spike firing during awake and anesthetized conditions. *J Pharmacol Sci.* 2018;136:172-176.
17. Purdon PL, Pierce ET, Mukamel EA, Prerau MJ, Walsh JL, Wong KF, Salazar-Gomez AF, Harrell PG, Sampson AL, Cimenser A, Ching S, Kopell NJ, Tavares-Stoeckel C, Habeeb K, Merhar R, Brown EN. Electroencephalogram signatures of loss and recovery of consciousness from propofol. *Proc Natl Acad Sci USA.* 2013;110:E1142-1151.
18. Gentet LJ, Avermann M, Matyas F, Staiger JF, Petersen CC. Membrane potential dynamics of GABAergic neurons in the barrel cortex of behaving mice. *Neuron.* 2010;65:422-435.
19. Kawaguchi Y, Kubota Y. GABAergic cell subtypes and their synaptic connections in rat frontal cortex. *Cereb Cortex.* 1997;7:476-486.
20. Bacci A, Huguenard JR, Prince DA. Functional autaptic neurotransmission in fast-spiking interneurons: a novel form of feedback inhibition in the neocortex. *J Neurosci.* 2003;23:859-866.
21. Vijayan S, Kopell NJ. Thalamic model of awake alpha oscillations and implications for stimulus processing. *Proc Natl Acad Sci USA.* 2012;109:18553-18558.
22. Vijayan S, Ching S, Purdon PL, Brown EN, Kopell NJ. Thalamocortical mechanisms for the anteriorization of alpha rhythms during propofol-induced unconsciousness. *J Neurosci.* 2013;33:11070-11075.
23. Flores FJ, Hartnack KE, Fath AB, Kim SE, Wilson MA, Brown EN, Purdon PL. Thalamocortical synchronization during induction and emergence from propofol-induced unconsciousness. *Proc Natl Acad Sci USA.* 2017;114:E6660-6668.
24. Bacci A, Huguenard JR. Enhancement of spike-timing precision by autaptic transmission in neocortical inhibitory interneurons. *Neuron.* 2006;49:119-130.
25. Feshchenko VA, Veselis RA, Reinsel RA. Propofol-induced alpha rhythm. *Neuropsychobiology.* 2004;50:257-266.

Figures

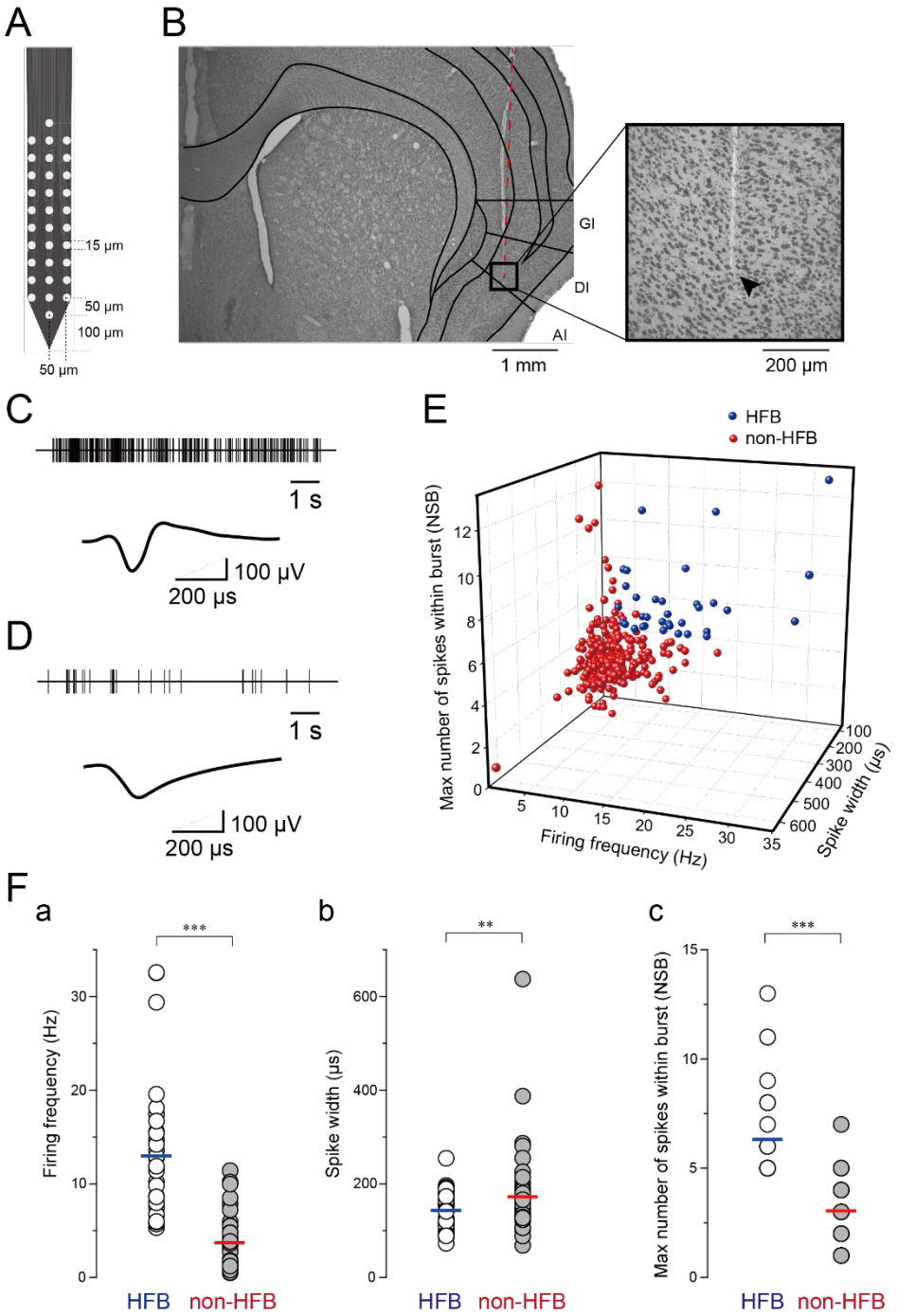

Figure 1. Extracellular recordings from IC. ***A.*** Arrangement of electrodes on the tip of the probe. ***B.*** A coronal Nissl-stained section with boundary lines. The boxed region is magnified on the right showing the tract of a recording electrode. The arrowhead indicates the most ventral site of the tract. ***C, D.*** Spontaneous activities of the IC neuron with a high firing rate with a burst (***C***) and the IC neuron firing at a low frequency without a burst (***D***) in the awake condition. The spikes are truncated. Averaged spike waveforms are shown in the bottom. Note the short spike width in (***C***) compared with that in (***D***). The neurons shown in (***C***) and (***D***) are classified as an HFB and a non-HFB, respectively. ***E.*** Distribution pattern of IC neurons in the scatter plot with three axes: firing frequency, spike width, and the maximum number of spikes within the burst (see Materials and Methods). According to the distribution pattern, IC neurons are divided into two categories: HFB with a high firing frequency (> 5 Hz) and large NSB max (≧ 5; red circles) and non-HFB that fire at low frequency (< 10 Hz, blue circles). Most HFB showed a short duration of spikes (< 150 μs). ***F.*** Comparison of spontaneous firing frequency (***a***), spike width (***b***), and maximum number of spikes within a burst (***c***) between HFB (n = 34) and non-HFB (n = 305). Horizontal bars indicate the mean. **: $P < 0.01$, ***: $P < 0.001$, Mann-Whitney U test.

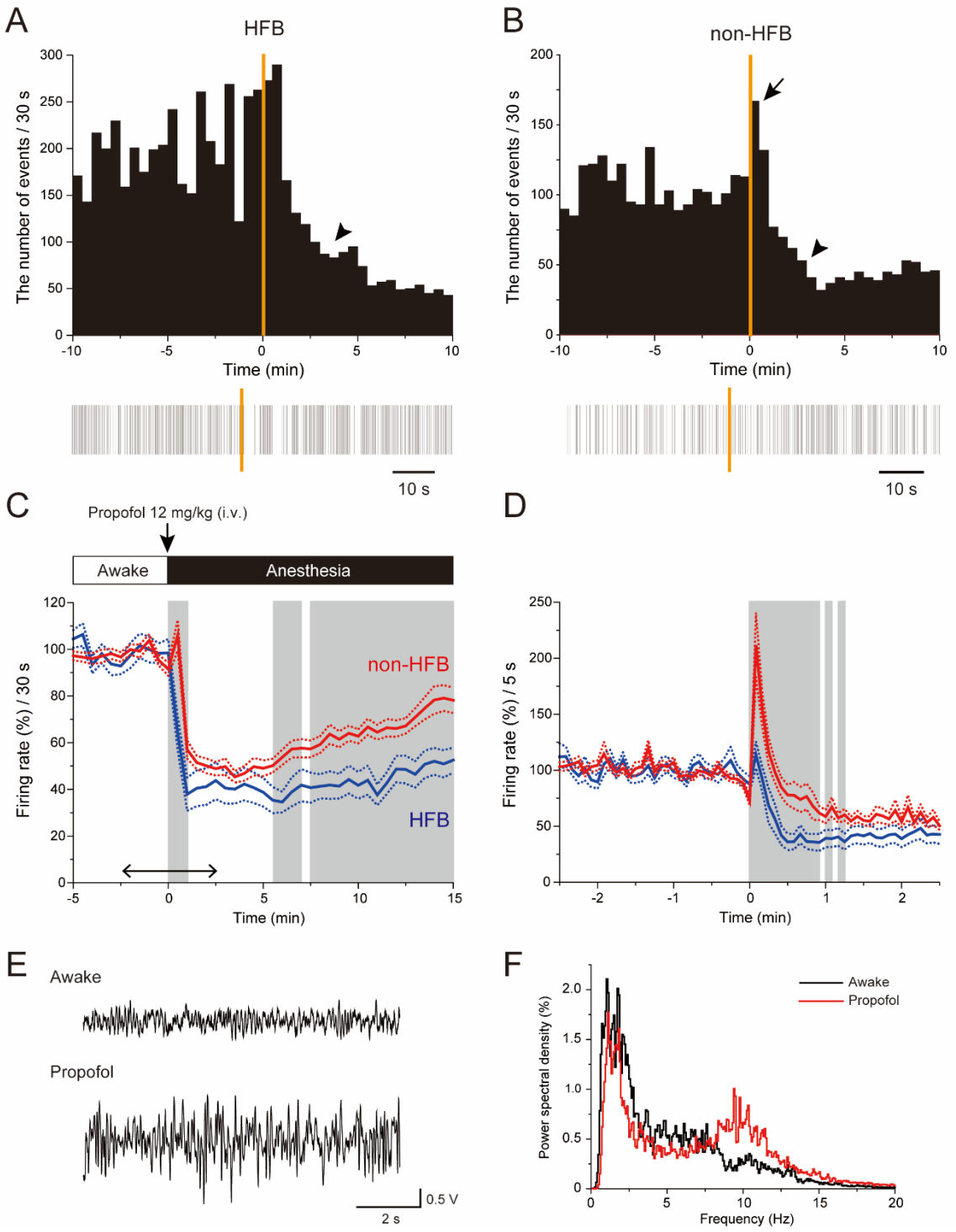

Figure 2. Propofol-induced changes in spike firing frequency in HFB and non-HFB. ***A, B.*** The number of spikes before, during, and after propofol injection to the tail vein (12 mg/kg) in an HFB (***A***) and a non-HFB (***B***) neuron. The bin width is 30 s, and the start point of injection is set at 0 (yellow lines). The bottom panels show spike firing in each neuron. ***C.*** Averaged number of spikes plotted against time obtained from 34 HFB (blue) and 304 non-HFB (red). Dotted lines indicate SEM. Shadows indicate significant differences between HFB and non-HFB ($P < 0.05$; Student's *t*-test). ***D.*** The time-expanded graph shown in ***C*** (double-headed arrow). ***E.*** An example of EEG under awake (upper) and propofol-induced anesthetized conditions (lower). ***F.*** Power spectral density analysis obtained from the neuron shown in ***E***. Note the enhancement of power spectral density between ~8 and 13 Hz.

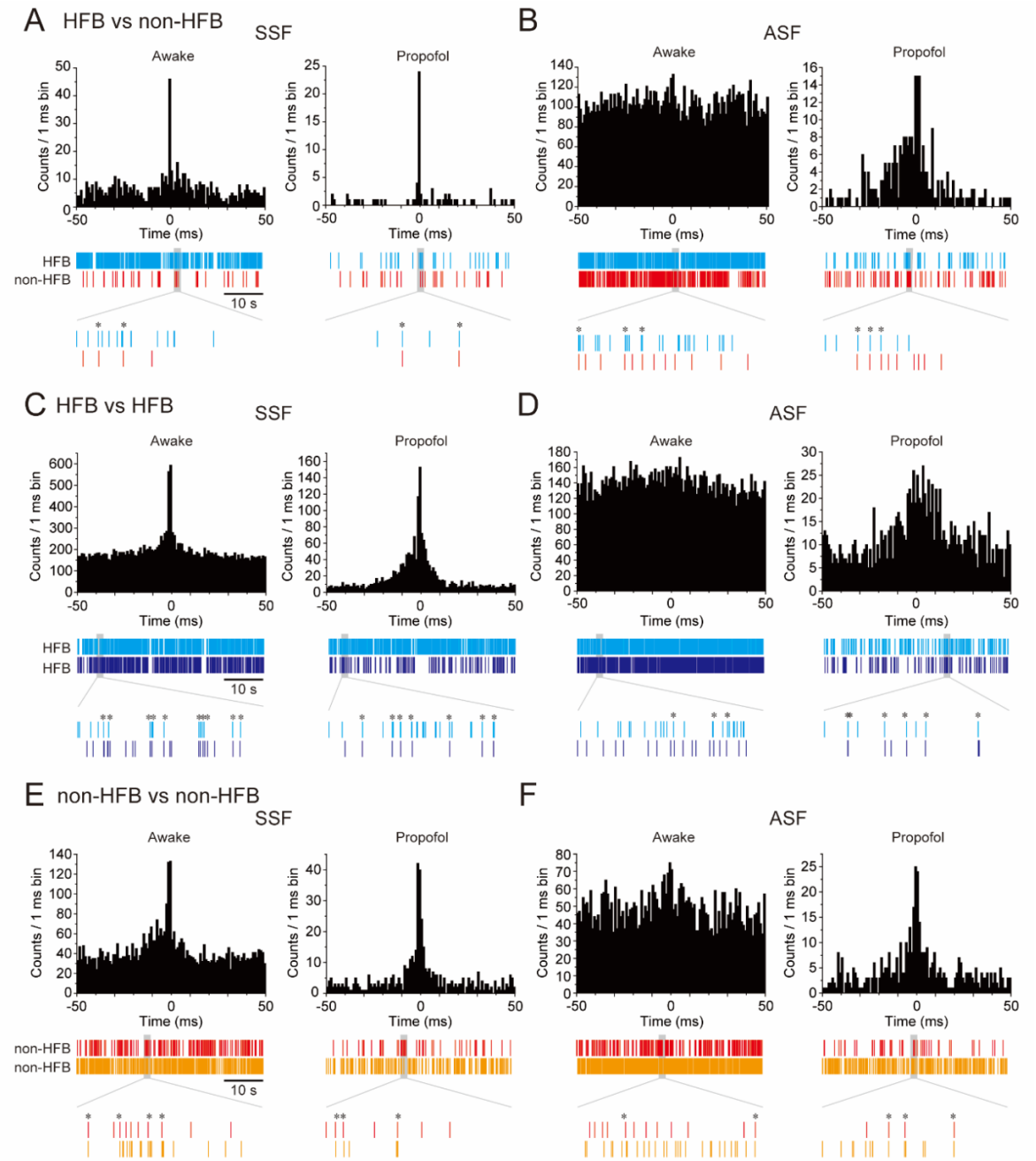

Figure 3. Propofol-induced effects on cross-correlograms between HFB and non-HFB (***A, B***), HFB and HFB (***C, D***), and non-HFB and non-HFB (***E, F***). ***A.*** An example of cross-correlograms exhibiting a prominent peak (SSF group) in the awake (***left***) and propofol-induced anesthetized conditions (***right***; see Materials and Methods) between HFB and non-HFB, whose spontaneous spike firing are shown in the middle panels. The bottom panels show time expanded spikelets of the shadowed areas in the middle panels. The awake and post-propofol states (30-570 s) show P/B ratios of 2.5 to 7.5, respectively. Asterisks on the bottom traces indicate simultaneous spike firing between the HFB and non-HFB. ***B.*** An example of cross-correlograms without a prominent peak in the awake condition (ASF group, see Materials and Methods). Note the emergence of a peak accompanied with a decrease in the baseline amplitude by propofol: P/B ratio is increased from 1.1 to 4.9. ***C, D.*** An example of cross-correlograms between HFB and HFB with (SSF; ***C***) and without a prominent peak in the awake condition (ASF; ***D***). Note the emergence of a peak accompanied with a decrease in the baseline amplitude by propofol. P/B ratios are increased from 1.8 to 5.6 in SSF (***C***) and 1.1 to 2.1 in ASF (***D***). ***E, F.*** An example of cross-correlograms between non-HFB and non-HFB with (SSF; ***E***) and without a prominent peak in the awake condition (ASF; ***F***). Note the emergence of a peak accompanied with a decrease in the baseline amplitude by propofol. P/B ratios are increased from 1.9 to 5.7 in SSF (***E***) and 1.2 to 4.0 in ASF (***F***).

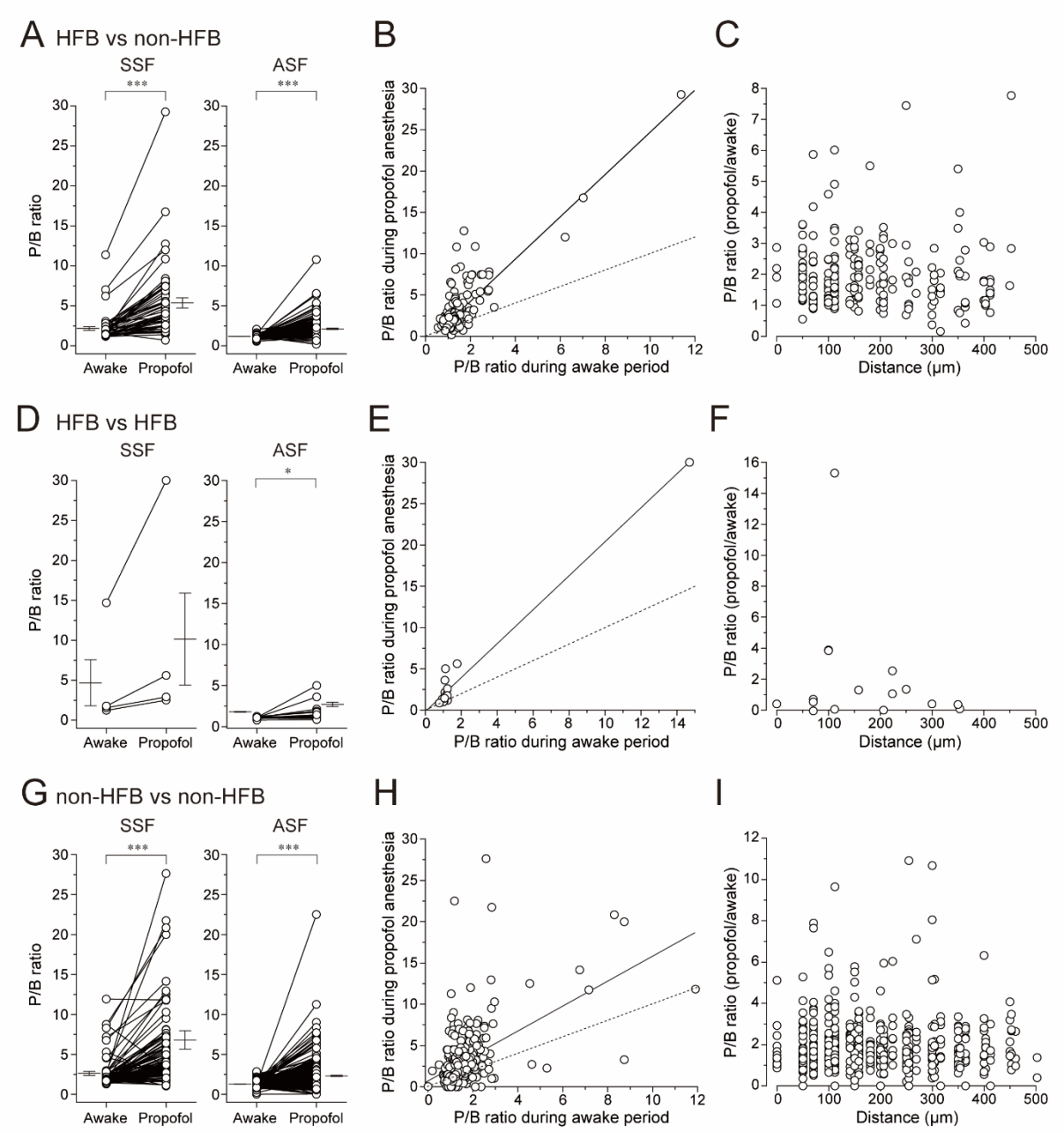

Figure 4. P/B ratios in the awake and propofol-induced anesthetized conditions obtained from HFB and non-HFB (***A-C***), HFB and HFB (***D-F***), and non-HFB and non-HFB pairs (***G-I***). ***A, D, G.*** Propofol-induced increase in P/B ratio in both SSF (***left***) and ASF groups (***right***) of HFB and non-HFB (***A***), HFB and HFB (***D***), and non-HFB and non-HFB pairs (***G***). Long and short horizontal bars adjacent to the plots indicate the mean and SEM, respectively. ***B, E, H.*** Relationship between P/B ratio during the awake and propofol-induced anesthetized conditions in HFB and non-HFB (***B***), HFB and HFB (***E***), and non-HFB and non-HFB pairs (***H***). The solid and dotted lines indicate the regression and identical lines, respectively. ***C, F, I.*** Relationship between the distance of neurons and the ratio (P/B ratio of propofol-induced anesthetized conditions divided by that of the awake condition) in HFB and non-HFB (***C***), HFB and HFB (***F***), and non-HFB and non-HFB pairs (***I***). *: $P < 0.05$, ***: $P < 0.001$; paired *t*-test.

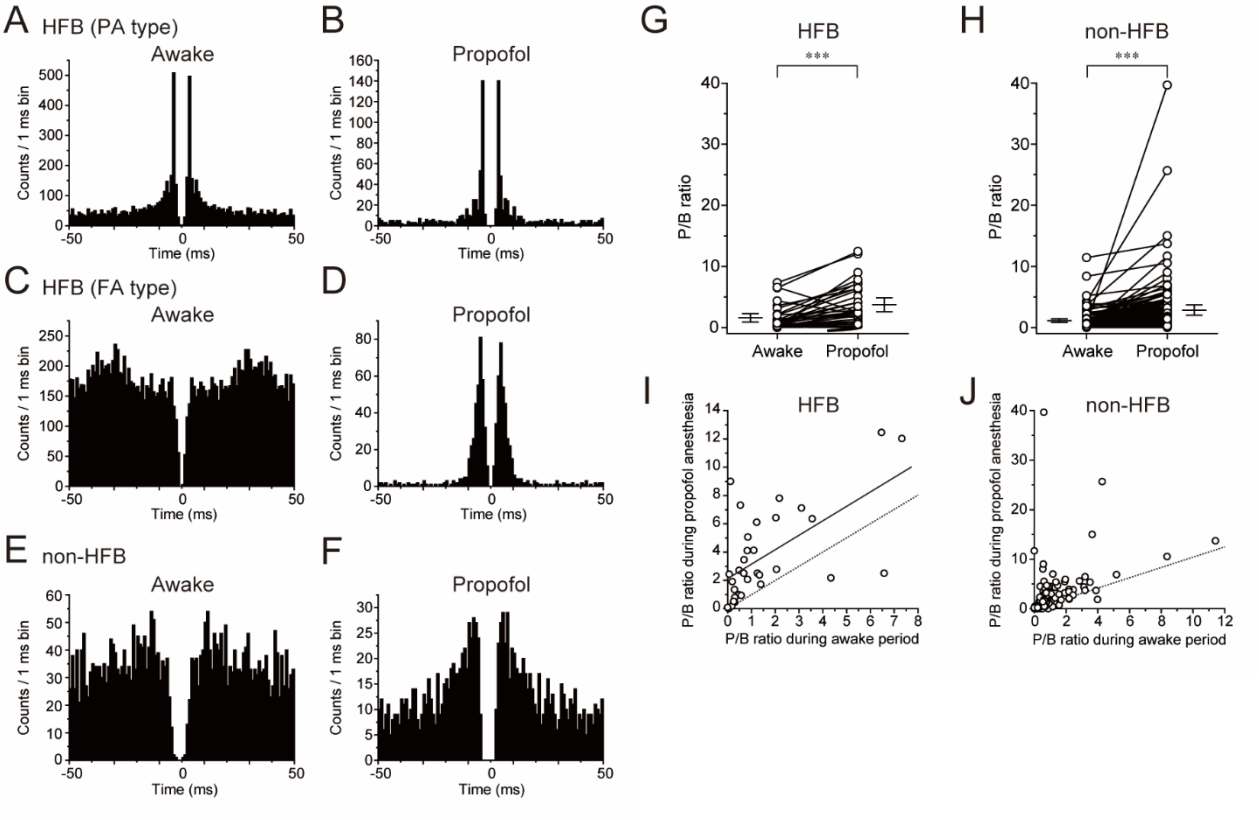

Figure 5. Auto-correlograms of HFB and non-HFB. ***A, B.*** An example of auto-correlograms of an HFB in the awake (***A***) and propofol-induced anesthetized conditions (***B***). This HFB exhibits prominent twin peaks around 0 ms. ***C, D.*** An example of auto-correlograms of an HFB that exhibit no significant peak in the awake condition. ***E, F.*** An example of auto-correlograms of a non-HFB that exhibit no significant peak in the awake condition. ***G, H.*** Propofol increases P/B ratio in both HFB (***G***) and non-HFB (***H***). Long and short horizontal bars adjacent to the plots indicate the mean and SEM, respectively. ***I, J.*** Relationship between P/B ratio during the awake and propofol-induced anesthetized conditions in HFB (***I***) and non-HFB (***J***).

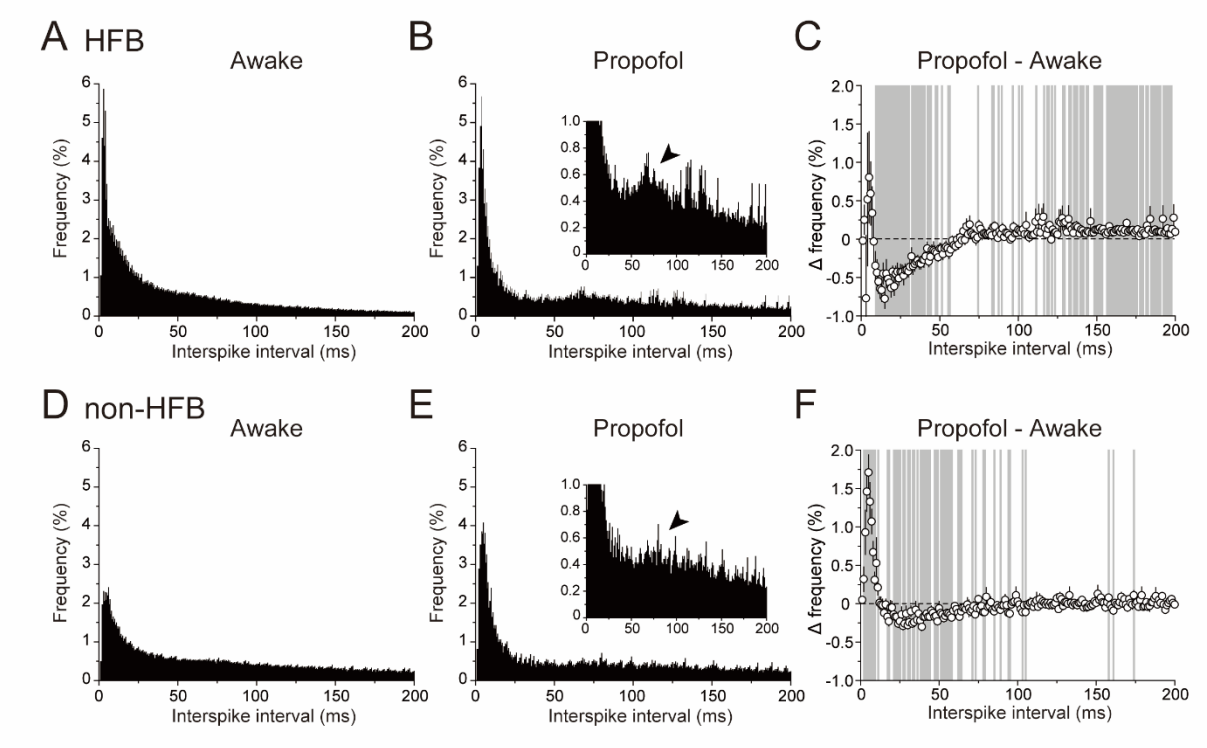

Figure 6. Distribution of the interspike intervals (ISI) in the awake and propofol-induced anesthetized conditions. ***A, B.*** ISI histograms of HFB (n = 34) in the awake (***A***) and propofol-induced anesthetized conditions (***B***). ***Inset:*** The frequency-expanded histogram showing the hump (arrowhead). ***C.*** Subtraction of the awake histogram (***A***) from that of the propofol (***B***). Shadows indicate significant differences between awake and propofol conditions ($P < 0.05$; paired *t*-test). ***D, E.*** ISI histograms of non-HFB (n = 305) in the awake (***D***) and propofol-induced anesthetized conditions (***E***). ***Inset:*** The frequency-expanded histogram showing the hump (arrowhead). ***F.*** Subtraction of the awake histogram (***D***) from that of the propofol (***E***). Shadows indicate significant differences between awake and propofol conditions ($P < 0.05$; paired *t*-test).

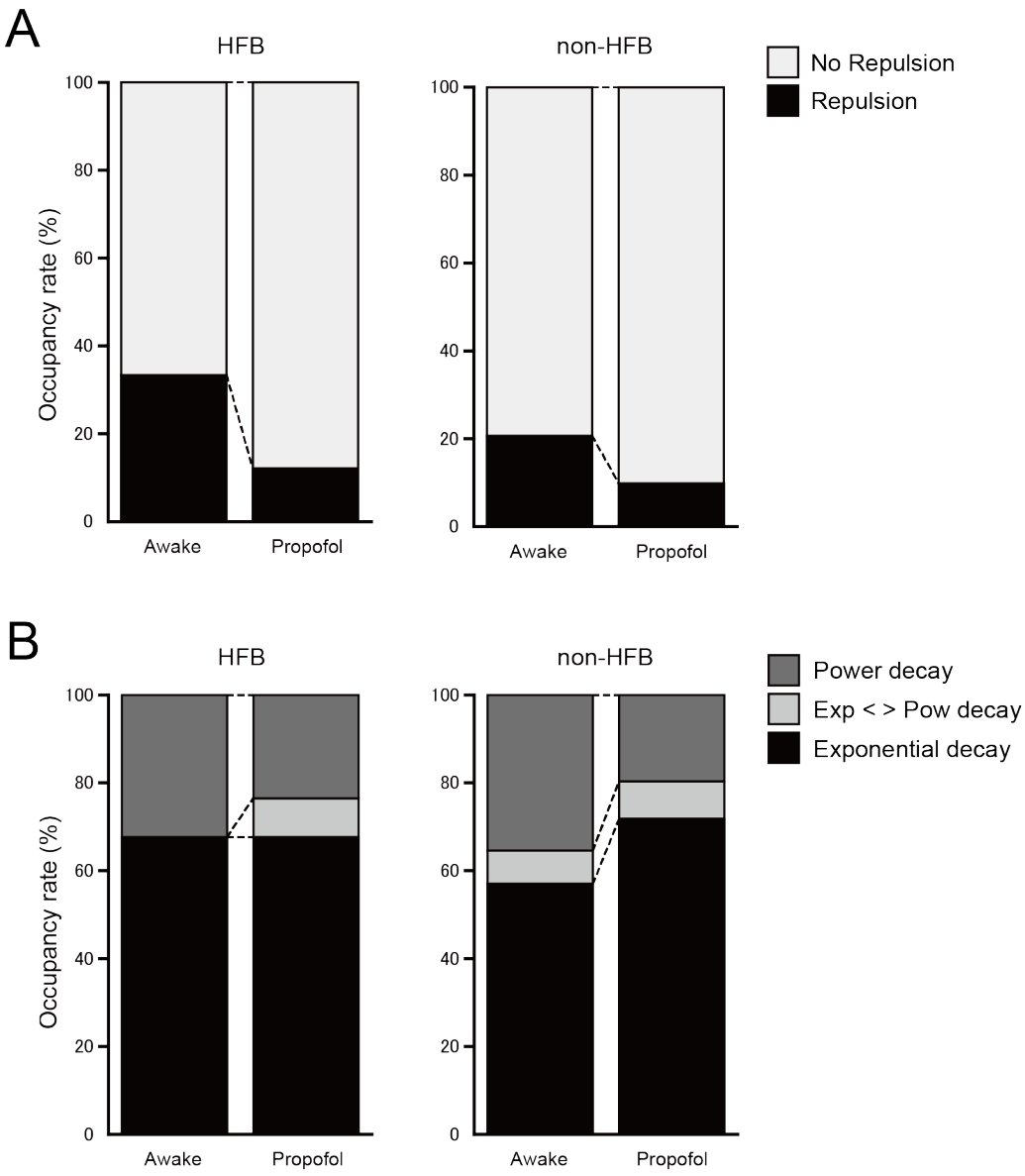

Figure 7. A. Population of HFB and non-HFB with or without repulsion. Propofol decreased the population of neurons with repulsion in both HFB and non-HFB. ***B.*** Population of HFB and non-HFB fitted with power (dark gray), exponential (black), or intermediate decay (light gray) under awake and anesthetized conditions. Propofol increased non-HFB fitted with exponential decay, whereas propofol had little effect on the population of HFB.